WAVELENGTH CALIBRATION AND INSTRUMENTAL PROFILES OF THE ISO-LWS GRATING

C. Gry[1], A. M. di Giorgio[2], R. Lorente[3] and E. Tommasi[4]

[1]ISO Data Centre, European Space Agency, Villafranca del Castillo, P.O. Box 50727, 28080 Madrid, Spain
[2]IFSI-CNR, Via Fosso del Cavaliere 100, 00162Roma, Italy
[3]XMM Science Operations Centre, INSA, Villafranca del Castillo, P.O. Box 50727, 28080 Madrid, Spain
[4]Agenzia Spaziale Italiana, via di Villa Patrizi 13, 00161 Roma, Italy

ABSTRACT

The in-flight wavelength calibration of the LWS grating is described, including the basic principles and calibration strategy, the calibration sources and observations, the unexpected time variation and the achieved accuracy (1/4 of a resolution element).

The study carried out to characterise the grating line profiles is presented. The line profiles are shown and compared to their Gaussian fits. The measured full-widths-at-half-maximum (i.e. the grating resolution) are a few % higher than the pre-launch values (0.29 μm for SW detectors and 0.6 μm for LW detectors), but this difference is expected to be eliminated by the transient correction, when available.

Key words: ISO – LWS – line profiles – wavelength calibration

1. WAVELENGTH CALIBRATION

1.1. Basic principles and calibration strategy

The LWS diffraction grating was mounted in a scanning mechanism which rotated through $\pm 7°$, allowing coverage of the extended range of wavelengths of each detector. The wavelength corresponding to each scanning position was determined by the grating angle θ_i (angle between the input aperture direction and the normal to the grating) and the detector angle θ_d (angle between the input aperture direction and the detector direction), which was a constant for a given detector.

$$\lambda = (sin\theta_i \; - \; sin(\theta_d - \theta_i))/Nk \qquad (1)$$

where N is the groove density of the grating (7.9 lines per mm) and k is the order: the grating was used in first order for the wavelength range 84-197 μm with the five long wavelength detectors LW1 to LW5, and in second order for the wavelength range 43-93 μm with the five short wavelength detectors SW1 to SW5.

In operations, the grating position was actually monitored via the engineering unit called LVDT (linear variable differential transformer). Therefore, once the ten detector angles were known, the wavelength calibration consisted in finding the relationship between the engineering units LVDT and the actual grating angle θ_i.

This was done by fitting a third order polynomial to a large data-base consisting of the measurements of emission line centroids in terms of LVDT units associated with the expected wavelengths of the lines for a number of calibration sources observed throughout the ISO mission.

Table 1. Lines from astronomical sources used for grating wavelength calibration. The source numbers correspond to the numbers used in Fig. 1.

line λ [μm]	det	LVDT mean(σ)	obs nb	sources
[OIII]51.81	SW1	1327(3)	171	1, 2, 3, 5, 6
[OIII]51.81	SW2	2783(3)	196	1, 2, 3, 5, 6, 7
[NIII]57.33	SW2	1993(2)	161	1, 2, 3, 5, 7
[NIII]57.33	SW3	3376(5)	152	3, 5, 7
[OI]63.18	SW2	1124(3)	88	3, 4, 5, 6, 7, 8
[OI]63.18	SW3	2584(3)	97	3, 4, 5, 6, 7, 8
[OIII]88.36	SW5	1579(3)	185	1, 2, 3, 5, 6, 7
[OIII]88.36	LW1	3142(4)	189	1, 2, 3, 5, 6, 7
[NII]121.89	LW2	2176(2)	7	7
[OI]145.53	LW3	1878(4)	76	3, 4, 5, 6, 8
[OI]145.53	LW4	3250(5)	80	3, 4, 5, 6, 7, 8
[CII]157.74	LW3	945(4)	90	3, 4, 5, 6, 7, 8
[CII]157.74	LW4	2374(3)	91	3, 4, 5, 6, 7, 8

1.2. Calibration sources and types of observations

The wavelength standards were mainly planetary nebulae and HII regions. They have been chosen so as to provide the largest possible sample of lines and so that several of them were visible from ISO as much as possible during the mission (see Table 1 and Figure 1). The lines used had to be strong enough to give good signal to noise and to be unresolved by the grating. The observations were performed weekly with end-to-end grating scans and provided measurements of seven different emission lines, spread between 51 μm and 158 μm, and appearing on two detectors each.

Note that there were no measurements for SW4 and LW5, as no strong lines were found in their wavelength range. However, the relationship is in principle independent of the detector and all measurements of all lines were used together.

Table 2. Detector angles adopted for wavelength calibration. The second line lists the shift of the new angle with respect to the angles measured on the ground.

	SW1	**SW2**	**SW3**	**SW4**	**SW5**	**LW1**	**LW2**	**LW3**	**LW4**	**LW5**
angle	67.80	58.74	49.71	40.73	31.72	63.26	54.29	45.27	36.275	27.32
shift	-.1	-.01	0.0	0.0	+.02	+.02	+.01	+.01	+.04	+.04

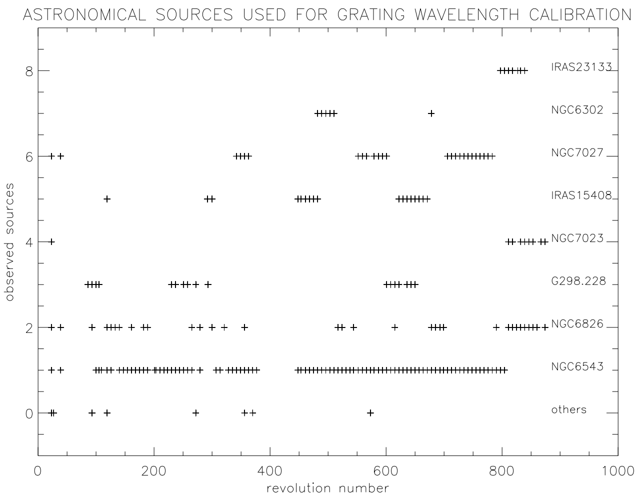

Figure 1. Main LWS grating wavelength standards observed during the mission. The gap between revolutions 378 and 442 corresponds to the period when LWS was not used because of a problem with the FP interchange wheel.

1.3. Detector angles

The wavelength calibration was first derived by adopting the detector angles measured before launch. Then the plot of the residuals (normalised differences between the expected wavelengths and the wavelengths derived from the LVDT with the polynomial relationship) showed systematic offsets for some detectors, suggesting that some of the detector angles had changed after launch. Therefore their values have been slightly adjusted, minimising the residual offsets for all detectors. The new angles used from pipeline version 6.0 onwards are listed in Table 2 together with the corresponding shifts relative to the pre-launch angles. The angle shifts for detectors SW4 and LW2 were adopted from the neighbouring detectors.

1.4. Time dependence

The stability of the system was checked by monitoring the measured LVDT at the line centres in the weekly observations. It is found to be remarkably stable for measurements performed close to the rest (central) position of the grating (LVDT $\sim$ 2100). But elsewhere, a little jump has happened in revolution 346. The jump was bigger the farther away the grating was from its rest position, and the jump had opposite signs for opposite angles (see Figure 2). After the jump, only a very slow drift was observed in the LVDT measurements. This jump implied that the relationship between grating angle and LVDT reading had changed on revolution 346 for an unknown reason and it was decided to derive a time-dependent wavelength calibration, which considers two distinct periods, i.e. pre- and post-revolution 346.

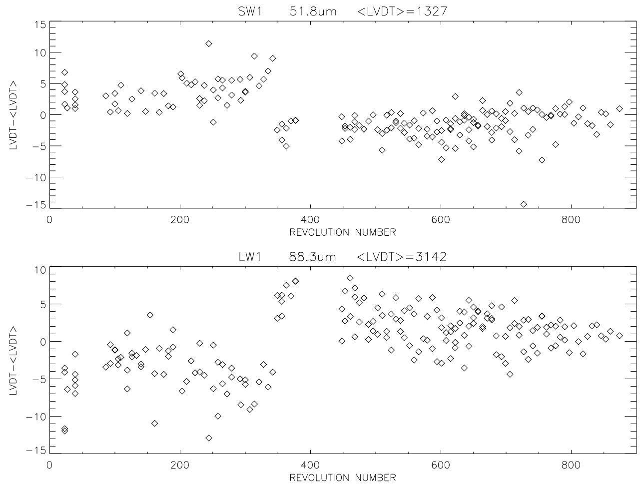

Figure 2. Deviation of the measured line centre (in engineering units LVDT) from the average value as a function of time, for two lines recorded at opposite grating directions relative to the rest position. 40 LVDT units correspond to 1 resolution element of the grating.

1.5. Assessment of the achieved wavelength accuracy

The accuracy of the grating wavelength calibration has been checked by measuring the central wavelengths of the lines observed in a large number (65) of auto-analysis results from observations of NGC7027, NGC6543, S106 and W Hya. This check has shown that in an individual observation the wavelength calibration is measured with an accuracy better than 1/4 of a resolution element (i.e. 0.07 μm for SW detectors and $0.15\,\mu$m or LW detectors). Only in one case were the errors slightly higher for an observation performed in a revolution just preceding the jump, when the noise on the LVDT reading was the highest.

2. RESOLUTION AND LINE PROFILES

2.1. PREPARATION OF THE DATA

The study of the grating profile has been performed with data obtained over the ISO lifetime for wavelength calibration (see Table 1 and Figure 1). In order to have an homogeneous sampling, only those data obtained with AOT L01, an oversampling of 8, 6 scans of the full grating range and the same number of forward and backward scans were used.

The data processing has been performed with the ISAP software. The standard processing of the selected observations is summarised by the following scheme:

- For each object we selected up to 20 observations well spread all over the mission.
- Each individual scan has been checked for the presence of glitches or any anomalous feature. Glitches have been removed and anomalous scans have been discarded.
- Each scan has been rebinned to 32 points per resolution element.
- Forward and backward scans have been averaged separately.
- In the cases of extended sources, the resulting scans have been corrected for the presence of fringes.
- The continuum has been fitted by a polynomial and subtracted off.
- The profile have been normalised so that the peak of all profiles was one.
- The resulting spectra have been re-centred to the laboratory wavelength, so that profiles from different velocity sources can be compared.

The products were thus one spectrum per scan direction per spectral line per detector per observation per object.

2.2. STABILITY OF THE LINE PROFILES

In order to define as general a profile as possible, parameters susceptible to inducing profile variations were looked for in a step-by-step approach. When a parameter had proved not to induce any significant variation, the profiles were averaged over this parameter for the subsequent study.

- **Stability with time.** All observations of the same line on the same detector for the same object have been plotted together to look for time variations. The peak to peak variations in the peak height of the line were as low as 2% for the strong lines and always less than 20% in the worst cases corresponding to the faintest lines used. No trend was found with time so these numbers are representative of the photometric accuracy of the LWS detectors. The variation of the line width with time was in general much smaller than the sampling interval of the observations (8 points per resolution element). We concluded that there are no significant time variations in the instrumental profiles.
- **Search for transient effects : comparison of forward and backward scans.** Slight differences do exist between the forward and backward scans of the same line from the same object due to transient or memory effects. In the short wavelength detectors the difference in the peak is always less than 2%, meanwhile in the long wavelength detectors it can be up to 6%. There is no trend with the flux level. In the line feet some broadening can be observed, in general on the short wavelength side for forward scans and on the long wavelength side for backward scans. The opposite case is also seen though, possibly due to errors in placing the continuum.

Because the effect is symmetrical when adding the forward and backward scans together, and because most of the differences between forward and backward scans are seen in the feet of the line, where they are confused with continuum features and thereby will be removed by the baseline subtraction process, our recommendation, as long as no formal transient correction is available, is to use both scan directions together. We have thus averaged forward and backward profiles for the rest of the study.

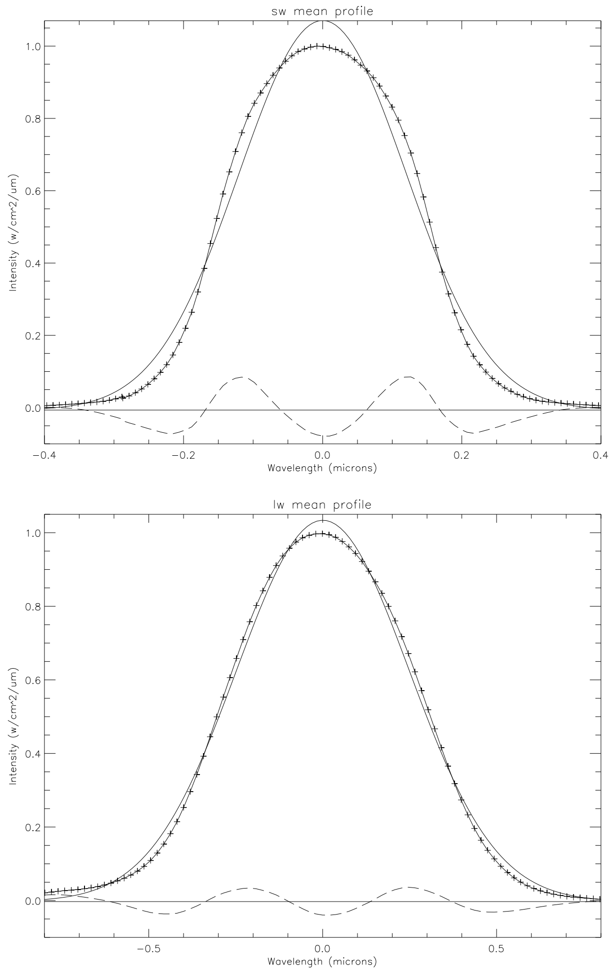

Figure 3. Measured grating profiles (plus signs) and comparison with a Gaussian fit (solid line). The residuals, i.e. the differences between the measured profile and the Gaussian fit, are also shown (dashed line). Up: profile for short wavelength detectors (SW1 to SW5) ; down: profile for long wavelength detectors (LW1 to LW5).

Table 3. Parameters of the computed grating profiles compared with the results of the Gaussian fits to the profiles.

	mean profile			Gaussian fit to the mean profile		
	FWHM (μm)	line flux (normalised) (to peak=1)	height	FWHM (μm)	line flux (normalised) (to peak=1)	height
SW detectors	$.308 \pm .005$	$.314 \pm .008$	1.00	$.283 \pm .009$	$.322 \pm .01$	$1.06 \pm .02$
LW detectors	$.611 \pm .014$	$.637 \pm .014$	1.00	$.584 \pm .015$	$.644 \pm .016$	$1.04 \pm .02$

– **Variation of line profile with object and detector.** In general the profiles show very little difference from object to object (the differences are less than 4%) and they show no significant differences between lines coming from different detectors.
  There is one exception with the clearly anomalous line at 57μm on detector SW2. It shows a strong asymmetry toward the short wavelengths for some objects. The asymmetry is clearly not real because it does not appear when the same line is observed with the detector SW3. It is not due to the detector either, as two other lines falling on SW2 (at 52μm and 63μm) do not show any anomaly. The 57μm line on detector SW2 has thus been excluded from the mean profile obtained by averaging all lines from all detectors in all objects.
– **Difference in line profiles from point and extended sources.** The profiles from extended sources and from point sources were kept separate to check whether off-centred emission was creating any distortion in the line profiles. The comparison of the mean profiles shows that, if anything, the profiles from the extended sources are more symmetrical and more similar to Gaussians than the point source profiles. We thus concluded that there is no distortion coming from the source extension or off-centring and we have averaged all profiles from point sources and extended sources together.

In conclusion, we have created two mean grating profiles (one for SW and one for LW detectors) which are the average of all lines listed in Table 1 except the 57μm line on SW2.

2.3. Characteristics of the profiles. Comparison to Gaussians.

When considering all the LWS optical elements and detector characteristics, the wavelength response function is not expected to be Gaussian. It is however always convenient when measuring a line intensity to be able to use a Gaussian approximation. Figure 3 shows the comparison of the measured mean profiles with Gaussian functions fitted to them. They also show the residuals, i.e. the differences between the profile and the Gaussian fit.
Table 3 lists the line flux, full width at half maximum and peak heights for the measured profiles and for the fitted Gaussian. This shows that the error made on the determination of the flux with a Gaussian fit is of the order of 2%. The line full-widths-at-half-maximum that we measure on our profiles are slightly larger than those measured before launch : 0.31 instead of 0.29 for the short wavelength detectors, and 0.61 instead of 0.60 for the long wavelength detectors. This is likely to be due to the broadening effect of transients.

2.4. Effect of a lower spectral sampling

The above study of the line profile has been conducted with the highest oversampling permitted in the observations, i.e. 8 points per spectral element. However, in AOT L01 and L02 four different oversamplings were permitted: 8, 4, 2 and 1. Following the Nyquist theorem, an oversampling of 2 or higher allows derivation of the line flux with a precision better than 5%. (A sampling of 1 point per spectral resolution element is clearly insufficient.) However, we would like to warn the user that a Gaussian fit performed to observations obtained with an oversampling of 2 or even 4 might result in a higher error than the one quoted above for an oversampling of 8. This is due to the fact that when a line is scanned quickly, the transient effects are more important and tend to broaden the line. This effect should be reduced once a transient correction is available.

ACKNOWLEDGEMENTS
This study has strongly benefited from the preliminary work of Bruce Swinyard and Sunil Sidher who designed the original wavelength calibration procedure and prepared the calibration software.